Green Chemistry

Cite this: *Green Chem.*, 2012, **14**, 1864

www.rsc.org/greenchem

COMMUNICATION

Nanoreinforced xylan–cellulose composite foams by freeze-casting†

Tobias Köhnke,[a,b] Angela Lin,[c] Thomas Elder,[d] Hans Theliander[b] and Arthur J. Ragauskas*[a]

Received 20th March 2012, Accepted 8th May 2012
DOI: 10.1039/c2gc35413f

Structured biofoams have been prepared from the readily available renewable biopolymer xylan by employing an ice-templating technique, where the pore morphology of the material can be controlled by the solidification conditions and the molecular structure of the polysaccharide. Furthermore, reinforcement of these biodegradable foams using cellulose nanocrystals shows potential for strongly improved mechanical properties.

In the current trend for a more effective utilization of biomass,[1] greater attention has been paid to the replacement of petroleum-based polymer foams with biopolymer foams based on renewable resources. The increased attention is not only based on issues of sustainability, but also on the fact that potential applications of high-porosity biopolymer based foams can be found in areas beyond those of conventional petroleum-based polymer foams due to the biocompatible and biodegradable properties of most biopolymers. Examples of potential applications for biopolymer based foams are kinetic energy absorbers, thermal and acoustic insulating materials, reinforcing platforms and scaffolds for nanocomposites, pharmaceutical and biomedical applications as drug carriers and tissue engineering scaffolds, and storage materials with high specific surface area.[2]

Among the different techniques used to create porous materials, freeze-casting has been shown to be a versatile, easily implemented, and promising technique. Freeze-casting involves freezing of a liquid suspension/solution followed by sublimation of the solidified phase under reduced pressure.[3] Particles/molecules in the suspension/solution are rejected from the moving solidification front, concentrated and finally entrapped between the growing solvent crystals. Consequently, the technique yields materials with porous structures where the pores are a replica of the solvent crystals. A variety of pore morphology can be obtained, depending on the choice of the solvent, formulation and the solidification conditions.[3] The freeze-casting process does not involve any chemical reactions, thus avoiding potential complications associated with by-products or purification procedures. Furthermore, the processing can be carried out with biocompatible liquid carriers such as water, which makes freeze casting highly attractive for the manufacture of materials for biomedical applications.[4]

Most studies dealing with freeze-casting involve inorganic particles,[3] but the technique can also be used in the formation of porous polymer and polymer–inorganic nanocomposites, as demonstrated by Zhang *et al.*[5] Previous studies have been performed on polysaccharides, such as agar,[6] chitosan,[7] alginate,[8] amylopectin,[9] and cellulose;[10,11] but to the authors' knowledge no one has investigated the potential in using the freeze-casting technique in the design of porous structures based on the second most abundant polysaccharide on earth, xylan.

Xylans constitute 25–35% of the dry biomass of woody tissues of dicots and lignified tissues of monocots and occur up to 50% in some tissues of cereal grains.[12] In terrestrial plants, xylans are heteropolymers, possessing a linear β-(1 → 4)-D-xylopyranan backbone substituted with a number of different side chains/groups, where L-arabinofuranosyl and 4-*O*-methyl-D-glucopyranosyl uronic acid units are most common. Due to issues of sustainability, increased attention has been focused on the engineered exploitation of xylans as biopolymer resources in the development of new materials. This interest is aided by the fact that xylans are readily available in residues and side-streams in the forestry/pulp and agricultural industry. Recent materials science innovations propose the use of xylan in films for food packaging, in coatings and as hydrogels.[13] The use of xylan in foam formulations would be another potential application for this biodegradable, readily available renewable biopolymer resource.

By using the freeze-drying method, free-standing xylan foams were successfully prepared without collapse and shrinkage. By comparing freeze-cast foam structures of xylan isolated from birch wood and wheat flour, it was discovered that the xylan molecular structure had a great influence on the pore morphology (Fig. 1a *vs.* 1b). The mechanism behind the development of different pore morphologies during freeze-casting is extremely complex and depends, according to Deville *et al.*,[14] on a large number of factors such as the freezing rate (or ice front velocity), the interfacial free energy between the particles, the water and the ice front, the particle size, distribution and content, the interaction of the particles with themselves, the

[a]*Institute of Paper Science and Technology, Georgia Institute of Technology, Atlanta, GA30332, USA. E-mail: art.ragauskas@ipst.gatech.edu*
[b]*Forest Products and Chemical Engineering, Department of Chemical and Biological Engineering, Chalmers University of Technology, SE-412 96 Gothenburg, Sweden*
[c]*Woodruff School of Mechanical Engineering, Georgia Institute of Technology, Atlanta, GA30332, USA*
[d]*USDA-Forest Service, Southern Research Station, 2500 Shreveport Highway, Pineville, LA71360, USA*
†Electronic supplementary information (ESI) available. See DOI: 10.1039/c2gc35413f

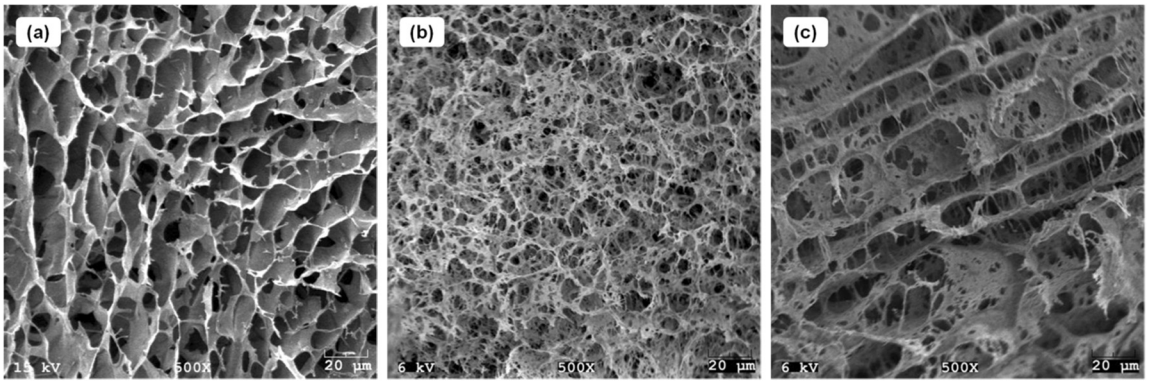

Fig. 1 SEM images of freeze-cast foams of glucuronoxylan from birch (a), and arabinoxylan from wheat flour with a degree of substitution of 0.6 (b) and 0.3 (c), illustrating the effect of xylan molecular structure on pore morphology.

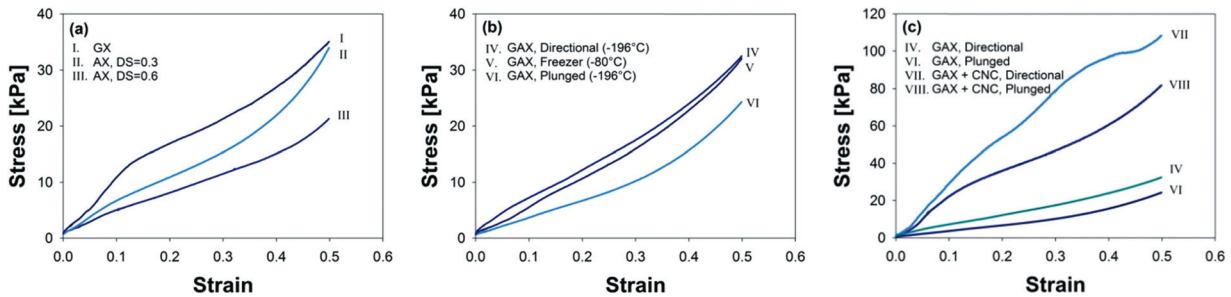

Fig. 2 Stress–strain curves of freeze-cast foams illustrating the effect of xylan molecular structure (a), solidification conditions (b), and cellulose nanocrystal reinforcement (25 wt% on GAX) (c). GX = glucuronoxylan, AX = arabinoxylan, GAX = glucuronoarabinoxylan, CNCs = cellulose nanocrystals, DS = degree of substitution.

anisotropic effects of the surface tension of ice, the buoyancy forces acting on the particles, the viscosity of the suspension/solution, the diffusion of the solute away from the interface, and the latent heat diffusion. The viscosity of the solution is a particularly important processing parameter in freeze-casting, since it determines the critical freezing front velocity at which particle trapping occurs during solidification.[4] It has been shown that the molecular structure of xylan has a major influence on different properties, such as solubility, aggregation, conformation in solution, viscosity, and interaction with other polysaccharides.[15] Considering these facts, it is plausible to assume that the pore morphology may be affected by the fine structure of xylan. To confirm this observation, the degree of arabinofuranosyl substitution of the wheat flour xylan was decreased by about 50% by an arabinofuranosidase treatment. As can be seen in Fig. 1b and 1c, this treatment induced formation of a more pronounced honeycomb-like structure, as was seen for birch xylan. The enzymatic treatment reduces the viscosity of the solution and increases the xylan–xylan interactions,[15] which clearly affects the velocity and structure of the solidification front.

The freeze-cast structures in Fig. 1 were tested for compressive properties in order to evaluate whether the difference in morphological structures (as a result of different xylan molecular structures) had an influence on the mechanical properties of the material. It is clearly shown that the morphology of the porous structure affects the mechanical properties of the freeze-cast material (Fig. 2a, Table 1). Consequently, the properties of freeze-cast xylan foams can be regulated by the choice of biomass for xylan isolation or by modifying the xylan molecular structure.

Table 1 Stress–strain data of the different foams presented in this study

Sample #	Composition[a]	Solidification method	Stress at 50% strain/kPa	Compressive modulus/kPa
I	GX	Plunged (−196 °C)	32 ± 4	79 ± 3
II	AX, DS = 0.3	Plunged (−196 °C)	35 ± 2	58 ± 4
III	AX, DS = 0.6	Plunged (−196 °C)	21 ± 3	39 ± 9
IV	GAX	Directional (−196 °C)	31 ± 1	57 ± 9
V	GAX	Freezer (−80 °C)	32 ± 1	41 ± 6
VI	GAX	Plunged (−196 °C)	25 ± 2	32 ± 6
VII	GAX + CNC (4 : 1)	Directional (−196 °C)	109 ± 3	285 ± 76
VIII	GAX + CNC (4 : 1)	Plunged (−196 °C)	83 ± 4	158 ± 44

[a] GX = glucuronoxylan, AX = arabinoxylan, GAX = glucuronoarabinoxylan, CNCs = cellulose nanocrystals, DS = degree of substitution.

The structural features of ice-templated materials may be controlled by exploiting the physics of ice formation. In particular

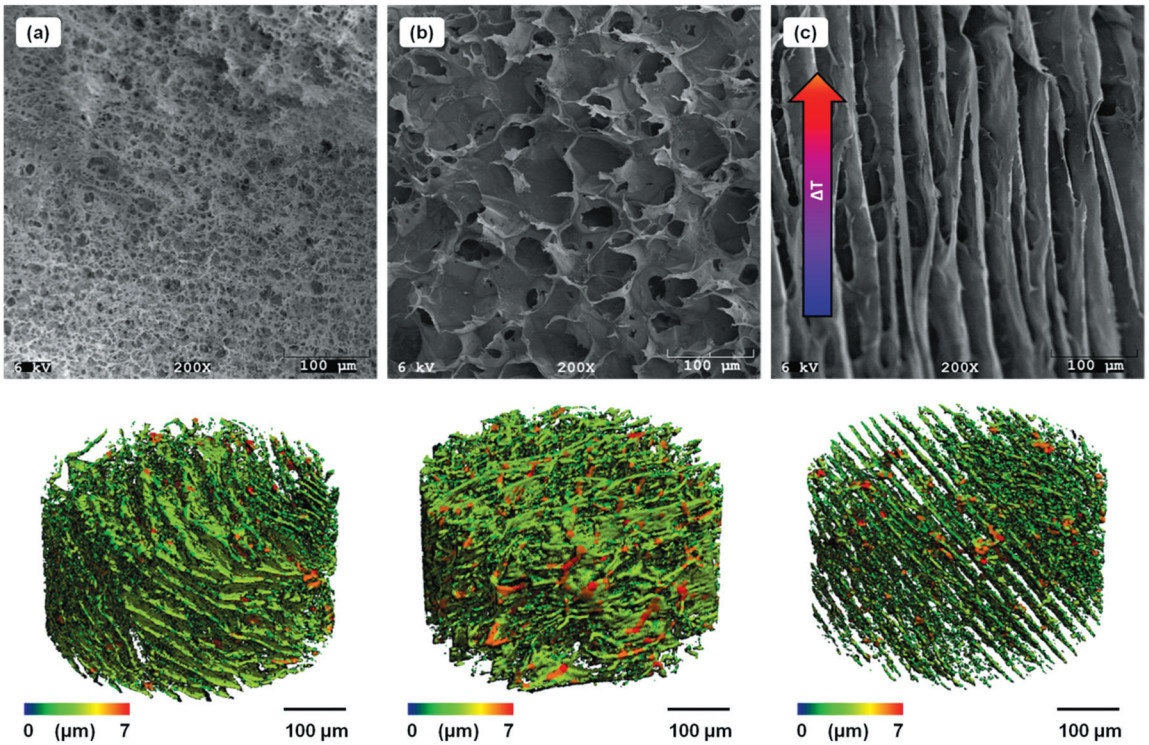

Fig. 3 SEM images and micro-CT images of freeze-cast foams of glucuronoarabinoxylan plunged in liquid nitrogen (−196 °C) (a), frozen in a freezer (−80 °C) (b), and unidirectionally frozen in liquid nitrogen (−196 °C) (c), illustrating the effect of solidification conditions on pore morphology.

the thickness of the ice crystals, and as a consequence the size of the templated pores, can be modified by increasing or decreasing the cooling rate during freezing. For fast cooling rates, supercooling becomes larger and the microstructure can be scaled down.[16] In other words, faster freezing rates produce finer microstructure. This is evident when comparing Fig. 3a and 3b, where glucuronoarabinoxylan (GAX) foams prepared at −196 °C and −80 °C are shown. The pores templated at the higher temperature are several times larger than those templated at the lower temperature.

The hexagonal ice crystals exhibit strong anisotropic growth kinetics, varying over about two orders of magnitude with crystallographic orientation.[17] The freezing process is easier for crystals whose preferred growth directions are parallel to the temperature gradient, and consequently the pores can be oriented depending on the solidification conditions used. For example, if only the bottom part of the vial containing the solution is in contact with liquid nitrogen, the solvent crystals are induced to grow vertically, along the direction of the imposed thermal gradient, which is clearly shown in Fig. 3c. Under those applied conditions, lamellae with a thickness of a couple of micrometers were formed, separated with a spacing of about 20–50 micrometers, as determined by SEM. When solutions were solidified without an applied temperature gradient, crystals could nucleate at any place and had no preferred growth direction, which resulted in structures with a random orientation of the pores (*cf.* Fig. 3b). If the whole vial containing the solution was inserted into liquid nitrogen, the initial freezing was not steady and the ice front orientation would also be completely random with no order. However, in a subsequent stage the ice-crystals would to some extent be stimulated to grow in a radial direction, from the outer surface to the centre regions, giving a final cylindrical sample structure with radially oriented pores (*cf.* Fig. 1 and 3a).

The xylan structures which possessed different porosities due to different solidification conditions were also investigated by microcomputed tomography (micro-CT) scanning (Fig. 3). The micro-CT images clearly confirm the morphologies seen in 2D SEM images. The CT-scanning data indicated a degree of porosity of 92–95% and a very high degree of pore interconnectivity (>99%), which was feasible considering the foam density of 25 kg m^{-3}.

The freeze-cast structures in Fig. 3 were tested for compressive strength properties in order to evaluate whether the difference in morphological structures (due to different solidification conditions) had an influence on the mechanical properties of the material (Fig. 2b, Table 1). It can be concluded that foams with a strong anisotropy of the porous structure in the loading direction show greater mechanical properties than porous foams achieved by non-directional freezing. It can also be concluded that samples possessing larger pores are stronger and stiffer than samples containing smaller pores.

In attempts towards mimicking structures and interactions in natural plant cell walls, cellulose nanocrystals (CNCs) have recently been used as reinforcement materials in xylan composite films and hydrogels.[18,19] Cellulose nanocrystals, derived sustainably from biomass by acid hydrolysis, represent a relatively new raw material that has attracted significant interest

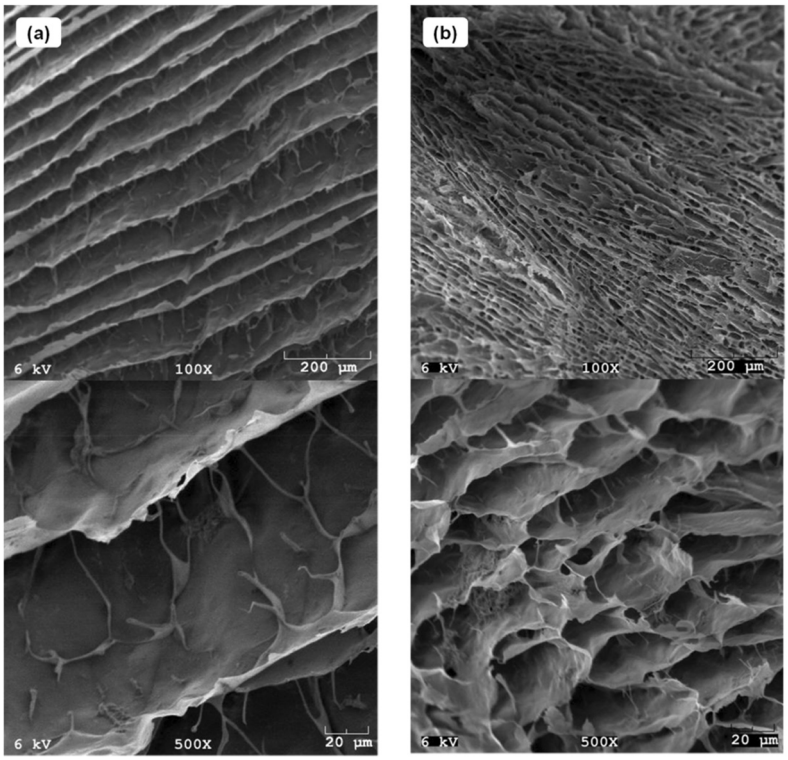

Fig. 4 SEM images of freeze-cast composite foams of glucuronoarabinoxylan and cellulose nanocrystals directionally frozen (a) and plunged (b) in liquid nitrogen (−196 °C).

in the last decade because of their impressive mechanical properties (modulus of about 140 GPa) and nanoscale dimensions (typically 5–20 nm in width and 100–300 nm in length).[20,21] If the crystals are obtained by sulfuric acid hydrolysis, negatively charged sulfonate ester groups are introduced on the crystal surfaces, leading to CNCs that are easy to disperse in water. These properties make them suitable for processing green nanocomposite materials from water based formulations. Furthermore, the xylan backbone has a high affinity to cellulose and will adsorb irreversibly on cellulosic surfaces,[15,22,23] a propensity which provides great opportunities for the use of cellulose as a reinforcement constituent in xylan based composites. To investigate if CNCs could be used as a strengthening agent in xylan foams, CNCs were prepared from microcrystalline cellulose by sulfuric acid hydrolysis. Atomic force microscopy (AFM) analysis of the obtained CNCs (*cf.* ESI†) revealed individual CNCs which possessed an average width (*i.e.* height) of 11 ± 2 nm and a length in the range of several hundreds of nanometers. The CNCs suspension also showed birefringence (*cf.* ESI†), which provided supporting evidence for the existence of rod-like CNCs.[20]

Reinforced foams were prepared by mixing the xylan solution with CNCs prior solidification. SEM imaging of the GAX–CNC-composites indicated that bridges were formed between the lamellae in the case of directional freezing, and distinctive cellular honeycomb-like pores were formed during quenching (Fig. 4), which was not as pronounced for pure GAX materials (Fig. 3). Obviously the content of CNCs affects the velocity and the structure of the solidification front. The fact that laminar and honeycomb-like structures can be prepared from pure CNC suspensions supports this observation.[10,11] The reinforced foams were tested for compressive strength (Fig. 2c, Table 1). Addition of 25 wt% CNCs increased the stress at 50% strain by about 250% and the modulus by about 400% for both directionally frozen and quenched materials. Even though the freeze-casting process has been used in a number of previous studies to obtain foams from other biopolymers than xylan, data on mechanical properties of these foams are lacking and quantitative comparisons of mechanical properties are consequently difficult to make. Furthermore, the mechanical properties of biofoams scale strongly with density and are dependent on the porous structure, where the latter is affected by the freeze casting process. Nevertheless, the compression strength of the presented xylan–CNC composite foam seems to be in the same order of magnitude as recently reported for micro-fibrillated cellulose (MFC) and starch foams.[2,24,25]

In summary, novel biofoams have been prepared from the readily available renewable biopolymer xylan by employing an ice-templating technique, where the pore morphology of the material is controlled by the solidification conditions and the molecular structure of the polysaccharide. Furthermore, reinforcement of these biodegradable foams using cellulose nanocrystals shows potential for strongly improved mechanical properties.

Experimental

Three different commercially available xylans were used in the study: birch glucuronoxylan[23] (GX) and oat spelt glucuronoarabinoxylan[18] (GAX), both obtained from Sigma-Aldrich, and wheat flour arabinoxylan[15] (AX) purchased from

Megazyme. Prior to use, all xylans were dialyzed (Spectra Por 2; MWCO: 12–14 kDa) against deionized and purified water in order to remove salts and low molecular weight fragments which could affect the freeze-casting process.

Cellulose nanocrystals (CNCs) were prepared by sulfuric acid hydrolysis of microcrystalline cellulose (Avicel PH-101 from Sigma Aldrich). In brief, 68.00 g (dry weight) of microcrystalline cellulose was mixed with 600 mL of a preheated (45 °C) 64% (w/w) aqueous H_2SO_4 solution under continuous stirring for 130 min. The hydrolysis reaction was stopped by adding an excess of deionized water followed by the removal of acidic solution by successive centrifugation until the supernatant became turbid. The sediment was collected and dialyzed (Spectra Por 2; MWCO: 12–14 kDa) until the pH of the solution became neutral. The content was sonicated (using a Model CU33 tapered ultrasonic cell disruptor horn from PGC Scientific, bearing a 12.7 mm tip and controlled with a GEX 500 ultrasonic processor, Sonics & Materials, with an output amplitude of 40%) in an ice bath for 6 min and centrifuged. The turbid supernatant, containing CNCs, was collected and the remaining sediment was again mixed with deionized water, sonicated and centrifuged to obtain additional CNCs; this procedure was repeated until the supernatant was clear. CNCs were obtained in 50% yield.

In order to investigate the influence of xylan molecular structure on the freeze-casted pore morphology, AX was treated with α-L-arabinofuranosidase (EC 3.2.1.55) from *Aspergillus niger* (CAZy GH51), purchased from Megazyme. The treatment was performed according to Köhnke *et al.*[15] In short, equal volumes of a 1% (w/v) AX solution and a sodium acetate buffer (100 mM, pH 4) containing 250 nkat g^{-1} AX of the enzyme were mixed and incubated at 40 °C for 24 h. After the treatment the solution was kept in a boiling water bath for 10 min in order to terminate the enzyme activity, dialyzed (Spectra Por 2; MWCO: 12–14 kDa) against deionized water, and finally freeze-dried.

The porous xylan foams were produced by freeze-casting of 2.5% (w/w) xylan solutions. Solutions were prepared by heating mixtures of xylan and deionized water to boiling under stirring. Suspensions for the xylan–CNC composite foams were prepared by mixing an equal volume of a 1.25% (w/w) CNC suspension and a 5% (w/w) xylan solution at room temperature. A solution/suspension volume of 1.00 mL was transferred into glass ampules, which were plunged into liquid nitrogen for 5 min. In the case of unidirectional freezing, only the bottom of the ampule was in contact with liquid nitrogen and vertical heat transfer was prevented by insulation of the ampule using polystyrene foam. Frozen samples were immediately put in a freeze-dryer to remove ice crystal templates by sublimation. The average diameter of the cylindrical samples after freeze-drying was 10 mm.

Prior to structural analysis the cylindrical samples were pulled into two pieces using two forceps. The pore morphology of the exposed inner surface parallel to the cylinder axis was studied after imaging of gold coated samples using a Hitachi S-800 field emission gun (FEG) scanning electron microscope (SEM) operated at 6 kV. A Scanco Medical was used to perform micro-computed tomography (micro-CT) scans on the specimens. Pieces of the full specimens were extracted to fit within a 2 mm ID sample scanning tube. Samples were imaged at the following scan settings: E = 45 kVp, I = 88 μA, integration time = 800 ms, pixel matrix 2048 × 2048, 2 μm voxel size. Raw data were automatically converted to 2D greyscale slice tomograms with a conebeam convolution backprojection algorithm. The 2D slice tomograms were globally thresholded to segment solid material from air/noise. The segmented 2D slices were then stacked to generate 3D binarized images of the material structure within a designated cylindrical volume of interest (VOI) within the scanned object. Pore interconnectivity was computed by inverting the solid and pore spaces and calculating the percent volume of the largest interconnected piece of the pore space.

Compressive tests were carried out on a Bose ELF 3200 using load cells of 4.9 N or 24.9 N. Due to a small surface roughness, a preload of approximately 0.05 N was applied to the cylindrical foam samples before initiating compression testing in the direction parallel to the cylinder axis. The compression rate of the cross-head was set to 0.1 mm s^{-1}. The modulus was calculated from the initial linear region (strain < 5%) of the stress–strain curves. Most materials showed a gradual transition from linear to non-linear stress–strain behavior with no pronounced horizontal plateau region, which consequently made it difficult to assign the yield point. Therefore, the materials were additionally compared by the stress at 50% strain. The samples were stored in a desiccator until analysis. Mechanical compression data were averaged over six specimens.

Acknowledgements

The authors gratefully acknowledge financial support from the Gunnar Nicholson Foundation.

Notes and references

1 A. J. Ragauskas, C. K. Williams, B. H. Davison, G. Britovsek, J. Cairney, C. A. Eckert, W. J. Frederick Jr., J. P. Hallett, D. J. Leak, C. L. Liotta, J. R. Mielenz, R. Murphy, R. Templer and T. Tschaplinski, *Science*, 2006, **311**, 484.
2 H. Sehaqui, M. Salajková, Q. Zhou and L. A. Berglund, *Soft Matter*, 2010, **6**, 1824.
3 S. Deville, *Adv. Eng. Mater.*, 2008, **10**, 155.
4 U. G. K. Wegst, M. Schecter, A. E. Donius and P. M. Hunger, *Philos. Trans. R. Soc. London, Ser. A*, 2010, **368**, 2099.
5 H. Zhang, I. Hussain, M. Brust, M. F. Butler, S. P. Rannard and A. I. Cooper, *Nat. Mater.*, 2005, **4**, 787.
6 H.-M. Tong, I. Noda and C. C. Gryte, *Colloid Polym. Sci.*, 1984, **262**, 589.
7 S. V. Madihally and H. W. T. Matthew, *Biomaterials*, 1999, **20**, 1133.
8 S. Zmorna, R. Glicklis and S. Cohen, *Biomaterials*, 2002, **23**, 4087.
9 A. J. Svagan, P. Jensen, S. V. Dvinskikh, I. Furó and L. A. Berglund, *J. Mater. Chem.*, 2010, **20**, 6646.
10 J. Lee and Y. Deng, *Soft Matter*, 2011, **7**, 6034.
11 R. Dash, Y. Li and A. J. Ragauskas, *Carbohydr. Polym.*, 2012, **88**, 789.
12 A. Ebringerová and T. Heinze, *Macromol. Rapid Commun.*, 2000, **21**, 542.
13 N. M. L. Hansen and D. Plackett, *Biomacromolecules*, 2008, **9**, 1493.
14 S. Deville, E. Saiz and A. P. Tomsia, *Acta Mater.*, 2007, **55**, 1965.
15 T. Köhnke, Å. Östlund and H. Brelid, *Biomacromolecules*, 2011, **12**, 2633.
16 S. Deville, E. Saiz, R. K. Nalla and A. P. Tomsia, *Science*, 2006, **311**, 515.
17 *Physics of Ice*, ed. V. F. Petrenko and R. W. Whitworth, Oxford University Press, New York, 1999.

18 A. Saxena, T. J. Elder, S. Pan and A. J. Ragauskas, *Composites, Part B*, 2009, **40**, 727.
19 M. A. Karaaslan, M. A. Tshabalala, D. J. Yelle and G. Buschle-Diller, *Carbohydr. Polym.*, 2011, **86**, 192.
20 S. J. Eichhorn, *Soft Matter*, 2011, **7**, 303.
21 E. C. Ramires and A. Dufresne, *Tappi J.*, 2011, April, 9.
22 T. Köhnke, H. Brelid and G. Westman, *Cellulose*, 2009, **16**, 1109.
23 T. Köhnke, K. Lund, H. Brelid and G. Westman, *Carbohydr. Polym.*, 2010, **81**, 226.
24 M. Pääkkö, J. Vapaavuori, R. Silvennoinen, H. Kosonen, M. Ankerfors, T. Lindström, L. A. Berglund and O. Ikkala, *Soft Matter*, 2008, **4**, 2492.
25 A. J. Svagan, L. A. Berglund and P. Jensen, *ACS Appl. Mater. Interfaces*, 2011, **3**, 1411.